

# Thermochemical Heat Storage Properties of Mechanically Activated $\text{Co}_3\text{O}_4$ -5 wt. % $\text{Al}_2\text{O}_3$ and $\text{Co}_3\text{O}_4$ -5 wt. % $\text{Y}_2\text{O}_3$ Composite Powders

A. Hasanvand, M. Pourabdoli\* and A. Ghaderi Hamidi

\*mpourabdoli@hut.ac.ir

Received: January 2019

Revised: April 2019

Accepted: August 2019

Advanced & Energy Storage Materials Lab., Department of Metallurgy and Materials Engineering, Hamedan University of Technology, Hamedan, Iran.

DOI: 10.22068/ijmse.17.1.45

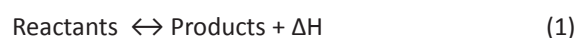
**Abstract:** The main problem with cobalt oxide as a thermochemical heat storage material is its slow re-oxidation kinetics. In addition, redox (reduction and oxidation) behavior of as-received  $\text{Co}_3\text{O}_4$  is degraded with increasing the number of redox cycles. To overcome this drawback,  $\text{Al}_2\text{O}_3$  and  $\text{Y}_2\text{O}_3$  were added to  $\text{Co}_3\text{O}_4$  and effect of mechanical activation time (2, 4, 8, and 16 h) on the redox behavior (weight change value/rate, redox reversibility, reduction and re-oxidation values, and particle morphologies) of  $\text{Co}_3\text{O}_4$ -5 wt.%  $\text{Al}_2\text{O}_3$  and  $\text{Co}_3\text{O}_4$ -5 wt. %  $\text{Y}_2\text{O}_3$  composites was investigated using thermogravimetry method. The composite powder were studied by SEM, EDS, and X-ray map analyses before and after redox reactions. Results showed that increasing the mechanical activation time improves the redox kinetics of  $\text{Co}_3\text{O}_4$ -5wt. %  $\text{Al}_2\text{O}_3$  in comparison with as-received  $\text{Co}_3\text{O}_4$ . Although, the alumina-containing samples, activated in short time showed the better redox kinetics than samples activated for longer times. It was found that increasing the activation time to more than 8 h for alumina-containing samples reduces the redox kinetics due to a decrease in the positive effect of  $\text{Al}_2\text{O}_3$  in controlling the particle size growth and sintering. In the case of  $\text{Co}_3\text{O}_4$ -5wt. %  $\text{Y}_2\text{O}_3$ , an increase in activation time generally reduced the redox kinetics. As a result, redox reactions in a 16 h-activated  $\text{Co}_3\text{O}_4$ -5wt. %  $\text{Y}_2\text{O}_3$  composite sample was completely stopped. In addition, results showed that weak performance of  $\text{Co}_3\text{O}_4$ -5 wt. %  $\text{Y}_2\text{O}_3$  is related to intensive sintering and growth of cobalt oxide particles during redox reactions.

**Keywords:** Cobalt oxide, Redox reactions, Reversibility, Thermochemical heat storage, Mechanical activation.

## 1. INTRODUCTION

One of the factors contributing to environmental pollution is the emission of greenhouse gases from fossil fuel consumption. The amount of these gases is increasing by the growth of industries and cars. According to industrialized nation's agreement, members are required to reduce the amount of greenhouse gases to control the air pollution. Therefore, changes in energy production and cleaner energy technologies is felt more than ever. These changes must be capable to reduce the fossil fuel consumption and greenhouse gases and, as a result, reduce environmental pollutions. One of these technologies that can reduce the environmental pollutions is Concentrated Solar Power (CSP) plants joint with Thermal Energy Storage (TES) technology. The most important use of TES is to overcome the mismatch between energy production and consumption especially in

technologies such as CSP plants that use the solar energy as a clean energy source. Solar energy is the most abundant source of renewable energy on the earth [1-5]. A description of the TES based on the chemical reduction and oxidation (redox) reactions, thermochemical energy storage (TCES), is derived from the following equation:



Equation (1) represents a balance between two or more reactive factors on one side, and products and enthalpy on the other side. In recent years, research interests in the field of TCES system have increased many folds due to its possibility to achieving a high energy density and capability of working at higher temperatures compared to other storage methods. The operating temperature range of the reversible reactions associated with proper redox pairs is between 400 and 1250 °C, which is

suitable for solar thermal power production. There are several important factors for the selection of a suitable material for thermochemical heat storage through redox reactions. These factors are thermodynamic conditions, energy storage capacity, material costs, reaction kinetics, toxicity, and behavior of materials during redox cycles [3, 6].

Attractive metal oxide redox pairs are those, which are capable of taking up and releasing gas-phase,  $O_2$ , at conditions relevant for generation of heat including e.g.  $Co_3O_4/CoO$ ,  $BaO_2/BaO$ ,  $Mn_2O_3/Mn_3O_4$ ,  $CuO/Cu_2O$ , and  $Fe_2O_3/Fe_3O_4$  among others. Among them, cobalt oxide has shown the most suitable behavior and has recently been used in cylindrical reactors for solar thermal energy storage. Multi-metallic redox oxides like Fe-Co- and Ca-Mn-based perovskites have also been tested recently. [7-9].

In  $Co_3O_4/CoO$  system,  $CoO$  and  $Co_3O_4$  oxides and their converting possibility into each other during reduction and re-oxidation reactions are used to thermal energy storage. The first stage of the cycle is endothermic reduction of  $Co_3O_4$  as follows [10]:



In the second stage, a  $CoO$  oxidation cycle occurs. This stage is accompanied by the release of heat.

The equilibrium temperature of the above reaction is about  $890^\circ C$ . This temperature is suitable for air-operated solar thermal tower plants that provide a temperature range of  $900 - 1000^\circ C$ . Among the various CSP technologies, air-operated solar thermal tower plants offer the potential for high temperatures and thus high thermodynamic conversion efficiencies together with the efficient use of air as a heat transfer medium. Despite the benefits of cobalt oxide, when it is subjected to redox cycles, its particles grow and sinter resulting in an increase in the oxygen diffusion distance and therefore reduction in the redox kinetics. To overcome this problem, various oxides including  $Fe_2O_3$ ,  $CuO$ , and  $Al_2O_3$  have been added to cobalt oxide. These additives improve thermochemical heat storage properties by preventing the growing and sintering of cobalt oxide particles [7, 10- 12].

Neises et al. [13] studied the effect of  $Al_2O_3$  and  $CuO$  additives on the cobalt oxide redox kinetics. Results showed that the addition of  $Al_2O_3$  has a greater effect on cobalt oxide redox kinetics than  $CuO$ . Pagkoura et al. [14] studied two different mixtures of cobalt oxide containing 10 and 4.5 wt. %  $Al_2O_3$ . These mixtures were prepared in a honeycomb shape and were subjected to thermal cycling. They found that although the addition of  $Al_2O_3$  decreases the heat storage capacity of cobalt oxide, it improves the redox kinetics of cobalt oxide by preventing the growth of cobalt oxide particles. A mixture of cobalt oxide with other elemental oxides such as Mn, Cu, Ni, and Mg oxides was used to thermal energy storage by Carrilo et al. [15]. They found the best yield in the cobalt-manganese oxides system. Agrafiotis et al. [16] used the cobalt oxide as a coating of silicon-carbide foam honeycomb cells and studied the properties of thermal energy storage in this system. They did not find a significant change in the improvement of thermal energy storage properties in cobalt oxide. However, cobalt oxide coating on silicon-carbide foams can be useful for storing thermal energy in long periods, because these foams produce extremely high oxide stability in thermal cycles.

Mechanical activation is a way to reduce the particle size (increasing the specific surface area) and uniform distribution of a secondary phase in a matrix [17]. Recently, Nekokar et al. [18] studied the mechanical activation effect on thermochemical heat storage properties of  $Co_3O_4/CoO$  system without any additive. Results showed that mechanical activation for more than 8 h, severely degrade the thermochemical heat storage properties of cobalt oxide. In fact, mechanical activation somewhat improves the redox kinetics of cobalt oxide in early redox cycles, but the redox behavior are degraded with increasing the number of cycles due to the growth and sintering of particles in comparison with non-activated sample. Another research by Nekokar et al. [19] showed that mechanical activation along with a secondary phase addition ( $Fe_2O_3$ ) improves the thermochemical heat storage properties of cobalt oxide. In fact, mechanical activation has a positive effect on the uniform distribution of secondary phase in cobalt oxide matrix and the prevention of the par-

ticle growth and sintering.

The current work investigates the effect of mechanical activation time on redox behavior (weight change/rate, redox reversibility, and particle morphology) of  $\text{Co}_3\text{O}_4$ -5 wt. %  $\text{Al}_2\text{O}_3$  and  $\text{Co}_3\text{O}_4$ -5 wt. %  $\text{Y}_2\text{O}_3$  composite powder. Two different metal oxides with similar valences ( $\text{Al}^{+3}$  and  $\text{Y}^{+3}$ ), different ionic radius ( $\text{Al}^{+3}$ : 0.0535 nm and  $\text{Y}^{+3}$ : 0.1019 nm), and different melting points ( $\text{Al}_2\text{O}_3$ : 2072 °C and  $\text{Y}_2\text{O}_3$ : 2425 °C) were used as additives to study the effect of type of additive on the redox behavior. In fact, novelty of this research is investigation of mechanical activation effect on redox behavior of cobalt oxide containing  $\text{Al}_2\text{O}_3$  and  $\text{Y}_2\text{O}_3$  as additives. To the best of the author's knowledge, these studies have not been reported until now.

## 2. MATERIALS AND METHODS

In this study,  $\text{Co}_3\text{O}_4$  (Merck, 99.5 wt. %, particle size < 10  $\mu\text{m}$ ),  $\text{Al}_2\text{O}_3$  (Fluka, 99.5 wt. %, particle size < 10  $\mu\text{m}$ ), and  $\text{Y}_2\text{O}_3$  (Merck, 99.5 wt. %, particle size < 10  $\mu\text{m}$ ) were used as raw materials. Alumina content of 5 wt. % as an optimum value was used according to previous publications [7, 8]. Also, yttria content of 5 wt. % was selected for comparability of results. Samples of  $\text{Co}_3\text{O}_4$ -5 wt. %  $\text{Al}_2\text{O}_3$  (CA) and  $\text{Co}_3\text{O}_4$ -5 wt. % of  $\text{Y}_2\text{O}_3$  (CY) were prepared by mixing the components. After mixing, they were mechanically activated for 2 (CA2), 4 (CA4), 8 (CA8), 10 (CA10) and 16 (CA16) hrs using a high-energy planetary ball mill (Retsch model PM100). A 150 mL steel container, steel balls (10 and 20 mm in diameter), a ball-to-powder weight ratio of 20, at rotational speed of 300-rpm under air atmosphere. A rest time of 15 minutes were taken after each h of ball milling to avoid the heating and undesirable reactions.

In thermogravimetric (TG) experiments, samples were poured into an alumina crucible and placed in a tube furnace. Then, redox reactions were carried out at a temperature range of 600-1200 °C at a heating and cooling rate of 10 °C / min, an air flow rate of 1340 ml/min. The sample weight was 3.8 g. The weight change in the samples during the redox reactions was recorded by a digital balance linked to a laptop. More details on the weight recording set up can be found in an ear-

lier work published by the authors [18]. To investigate the morphology and chemical composition of powders, scanning electron microscopy (LMU VEGA//TESCAN) equipped with Energy-dispersive Spectroscopy (EDS) was used. Average particle size of the samples was determined by SEM images and MIP4 software.

## 3. RESULTS AND DISCUSSIONS

### 3.1. As-Received Cobalt Oxide Redox Behavior

Fig. 1 shows the TG curve of the as-received  $\text{Co}_3\text{O}_4$  in three redox cycles. As it is shown, the weight loss value in the first, second and the third cycle is 4.2, 3.4, and 1.8 wt. %, respectively indicating a decrease in oxygen removal capacity by increasing the number of cycles. Weight loss and weight increase are the same only in the first cycle and they are different in the second and the third cycle. In general, it is clear that redox behavior of as-received  $\text{Co}_3\text{O}_4$  is non-regular and is degraded with increasing the number of redox cycles.



Fig. 1. TG curve of as-received  $\text{Co}_3\text{O}_4$  during three redox cycles.

As said earlier, the main drawback of cobalt oxide as a thermochemical heat storage material is slow redox kinetics in high number redox cycles. It is seen that redox reversibility of as-received cobalt oxide (Fig. 1) is stopped after three cycles. In this research,  $\text{Al}_2\text{O}_3$  and  $\text{Y}_2\text{O}_3$  additives along with mechanical activation were used to improve the redox behavior of  $\text{Co}_3\text{O}_4$ .

### 3.2. Effect of Mechanical Activation on $\text{Co}_3\text{O}_4$ -5wt. % $\text{Al}_2\text{O}_3$ Composite Powder Redox Behavior

Fig. 2 shows the TG analysis of  $\text{Co}_3\text{O}_4$ -5wt. %  $\text{Al}_2\text{O}_3$  samples that were activated for various

times. The results is an evidence that mechanical activation along with  $\text{Al}_2\text{O}_3$  addition have improved the redox behavior of  $\text{Co}_3\text{O}_4$ . Useful data of Fig.2 derived and recorded in Table 1. According to Fig. 2 and Table 1, redox reversibility, weight change, and weight change rate of CA samples have improved in many cases in comparison with the as-received cobalt oxide.

### 3.2.1. Weight Change During Reduction and Re-Oxidation

As it is shown in Table 1 and Fig. 2, the weight loss (oxygen desorption value) in CA2 and CA4 samples is increasing with the increase in the redox cycles. For example, CA2 sample in the first, second, and third cycle desorbed 2.63, 4.73, and 5.26 wt. % oxygen, respectively. Oxygen desorption value in CA8 sample is relatively constant in three redox cycles indicating the regular redox cycles. In CA10 sample, oxygen desorption values are less than other samples. CA16 performance in cycle one is better than other cycles probably due to smaller particle size.

According to Table 1, oxygen desorption and absorption values in a cycle for a sample almost are the same. It means that unlike as-received cobalt oxide sample, alumina-containing samples show reversibility in each individual cycle.

If only the second and the third cycle are considered, it is seen that with increasing the redox cycles, desorbed oxygen value is increasing in all samples. Increasing the oxygen desorption value in each sample by increasing the redox cycles is most likely due to the decomposition of  $\text{CoO} \cdot \text{Al}_2\text{O}_3$  spinel phase during redox cycles that is formed during mechanical activation. Reduction in oxygen desorption value by increasing the activation time is also due to an increase in sintering and particle growth by increasing the activation time. In fact, mechanical activation leads to an increase in sample specific surface area that increases the particles sintering during redox process resulting in an increase in the oxygen diffusion distance. That is equivalent to increasing the reaction time or reducing the reaction speed [18-20].

According to Table 2, it is seen that alumina addition and mechanical activation have improved the reduction and re-oxidation kinetics of cobalt oxide in comparison with as-received cobalt oxide. Al-

though, the samples activated for short times, show the faster redox kinetics than samples activated for longer times. That is in agreement with Nekokar et al. [18] findings that showed mechanical activation for long times degrades the TECS properties.



**Fig. 2.** TG analyses of CA samples (activated for 2, 4, 8, and 16 h) during three redox cycles.

From Fig. 3 and Table 2, it is clear that average particle size of CA16 sample is less than other samples. Therefore, the high oxygen desorption value by CA16 in cycle one can be due to its high surface area. But, in high number redox cycles, the oxygen desorption value of CA16 is decreased and reached to less than oxygen desorption value



of CA2, CA4, and CA8 samples due to a positive effect of activation time on particle sintering. Mechanical activation not only promotes the particles growth and sintering, but also facilitates the formation of complex compositions that may decompose hardly during redox reactions. It is concluded that increasing the mechanical activation time decreases the oxygen desorption value due to an increase in the particle size during redox reaction and formation of hardly decomposable compounds. On the other hands, mechanical activation results in a more uniform distribution of the additives in the matrix as it is seen in SEM images (Fig. 3 and Fig.4). According to Fig.3 and Fig.4, there is a decrease in the agglomerate size with an increase in the activation time.

### 3.2.2. Weight Change Rate During Reduction and Re-Oxidation

We consider only the results of cycle two and cycle three because the mechanically activated samples in cycle one are not stable and show irregular behavior. According to Table 1, weight loss rate (reduction step) of CA2, CA4, and CA8 samples is in the range of 0.22-0.37 wt. % per minute during the second and third cycle. Weight loss rate of CA16 is less than other samples. In general, increase in activation time from 2 to 8 h did not have a significant effect on the rate of weight loss, but an increase of activation time to 16 h led to a significant decline in the weight loss rate. Reasons

for this are similar to the discussion mentioned for weight loss. Therefore, increasing the activation time to more than 8 h reduces the thermochemical heat storage properties of  $\text{Co}_3\text{O}_4$ . In the other words, increasing the activation time to more than 8 h decreases the positive effect of  $\text{Al}_2\text{O}_3$  addition in controlling the particle size and sintering. Also, it probably facilitates the formation of compounds that hardly decompose during redox reactions.

Table 1 shows that both of re-oxidation value and re-oxidation rate in all of CA samples have significantly improved in comparison with as-received cobalt oxide. It means that  $\text{Al}_2\text{O}_3$  addition along with mechanical activation especially up to 8 h was capable to improve the re-oxidation behavior. Although, the rate of oxygen absorption is less than the rate of oxygen desorption in all samples. In addition, the rate of weight increase during first cycle for all samples is lower than the second and third cycles. It is noteworthy that CoO melting point is 1933 °C, while  $\text{Co}_3\text{O}_4$  melting point is 895 °C. In the reduction step, a CoO layer is formed on  $\text{Co}_3\text{O}_4$  particles, but the layer that forms in the re-oxidation step is  $\text{Co}_3\text{O}_4$  on CoO layer. Therefore, due to the low melting point of  $\text{Co}_3\text{O}_4$ , a continuous layer can be formed on CoO phase and therefore, particle sintering in re-oxidation step take place easier than reduction step. The larger particle size, the longer is the oxygen sorption time. In addition, the presence of un-reacted cobalt oxide layers gradually reduces the absorption/desorption capacity and ultimately complete

**Table 1.** Weight change and it's rate during first to third redox cycles of  $\text{Co}_3\text{O}_4$ -5 wt.%  $\text{Al}_2\text{O}_3$  derived from Fig. 2

| Sample code                         | Weight change<br>wt. % |      |         |      |         |      | Weight change rate<br>(wt.% / min) |      |         |      |         |      |
|-------------------------------------|------------------------|------|---------|------|---------|------|------------------------------------|------|---------|------|---------|------|
|                                     | Cycle 1                |      | Cycle 2 |      | Cycle 3 |      | Cycle 1                            |      | Cycle 2 |      | Cycle 3 |      |
|                                     | Red                    | Oxid | Red     | Oxid | Red     | Oxid | Red                                | Oxid | Red     | Oxid | Red     | Oxid |
| As-received $\text{Co}_3\text{O}_4$ | 4.20                   | 4.20 | 3.40    | 2.2  | 1.8     | 0    | 0.37                               | 0.18 | 0.11    | 0.11 | 0.05    | 0    |
| CA2                                 | 2.63                   | 2.63 | 4.73    | 4.73 | 5.26    | 5.26 | 0.33                               | 0.26 | 0.32    | 0.39 | 0.35    | 0.26 |
| CA4                                 | 2.50                   | 2.50 | 4.40    | 4.40 | 5.32    | 5.32 | 0.42                               | 0.23 | 0.22    | 0.31 | 0.37    | 0.32 |
| CA8                                 | 5.00                   | 5.00 | 4.50    | 4.50 | 5.00    | 5.00 | 0.33                               | 0.41 | 0.30    | 0.30 | 0.33    | 0.29 |
| CA16                                | 4.50                   | 4.50 | 3.16    | 3.16 | 3.42    | 3.42 | 0.35                               | 0.45 | 0.22    | 0.20 | 0.31    | 0.26 |

stopping of the redox reversibility [8].

Therefore, it is concluded that addition of alumina to cobalt oxide and mechanical activation have improved the weight change rate and re-oxidation value of cobalt oxide in comparison with as-received  $\text{Co}_3\text{O}_4$ .

### 3.2.3. Particle Size and Morphology

The SEM images of CA2, CA8, and CA16 samples before and after three redox cycles are shown in Fig. 3. The figure shows that the particle size is decreased with the increase in the activation time before redox process. Average particle size of CA2, CA8, and CA16 samples before redox process is 0.95, 0.82, and 0.63  $\mu\text{m}$ , respectively, while it reaches to 2.50, 4.20, and 3.50 after three redox cycles (Table 2). It means that with the increase in the activation time increasing time to 8 h, the average particle size after redox has increased. It is clear that although the average particle size of CA2 before redox is larger than the average particle size of CA16, but after the third redox cycle, the average particle size of CA2 is smaller than CA16. It means that a

long mechanical activation time increases the particle size after redox reactions.

Average particle size of CA16 sample is smaller than that of CA8 sample after redox process. The following two reasons are provided for the difference in behavior: Reason one, the average particle size of CA16 sample is smaller than other two samples before redox, and therefore it requires long cycles for growth and sintering in comparison with CA8 samples. Reason two,  $\text{Al}_2\text{O}_3$  has dispersed more uniformly than other samples in the cobalt oxide matrix due to higher activation time. These two factors have decreased the sintering of CA16 sample in comparison with CA8 sample.

**Table 2.** Average particle size of CA samples before and after three redox cycles

| Sample code | Average particle size ( $\mu\text{m}$ ) |                      |
|-------------|---|----------------------|
|             | Before redox                            | after 3 redox cycles |
| CA2         | 0.95                                    | 2.50                 |
| CA8         | 0.82                                    | 4.20                 |
| CA16        | 0.63                                    | 3.50                 |

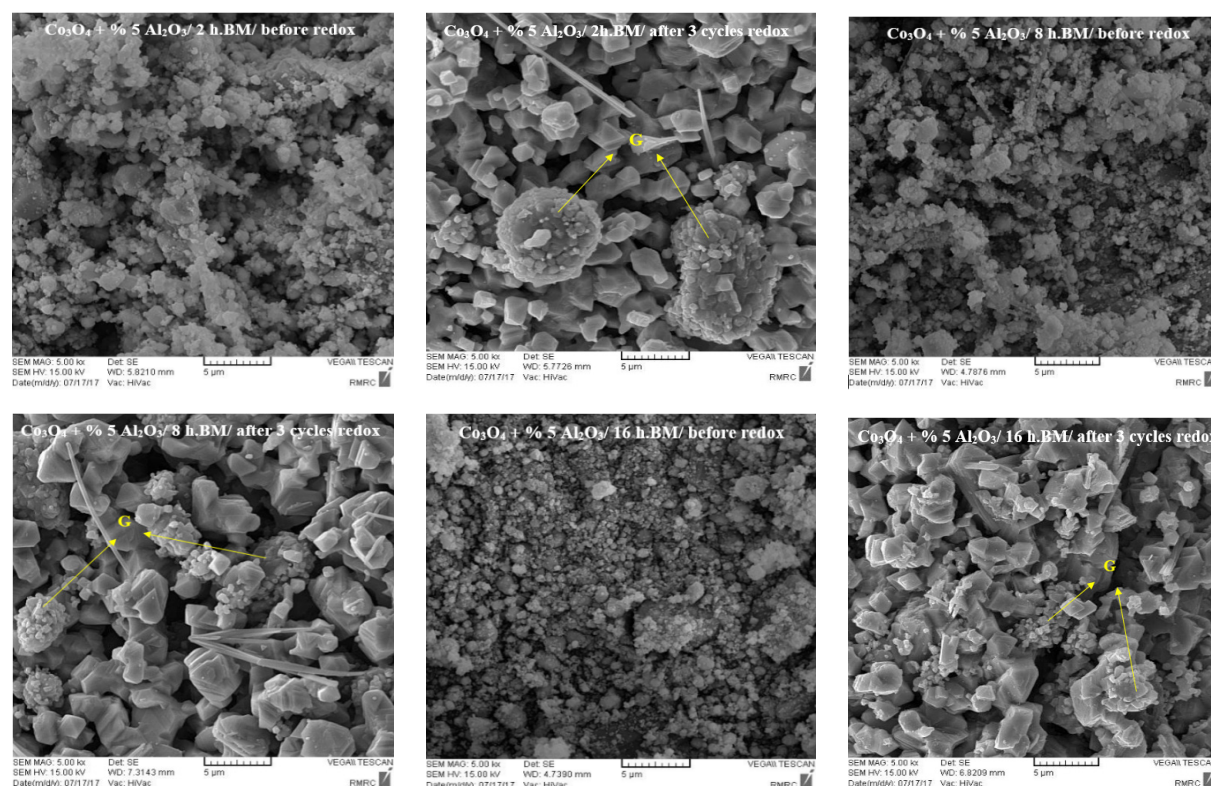


**Fig. 3.** SEM images of CA2, CA8, and CA16 samples before and after three redox cycles.

### 3.2.4. Chemical Analysis of Particles

In Fig. 3 some agglomerated particles are seen that are formed from a set of fine particles (marked with G). These agglomerated particles are present in all of the samples after redox. Only difference is their size that has decreased with the increase the activation time. For further investigation and identification of possible compounds formed between cobalt oxides and  $\text{Al}_2\text{O}_3$ , CA8 sample was analyzed by EDS and X-ray map analyses.

According to X-ray map and EDS analysis presented in Fig. 4, the agglomerated particles (A and B points) are rich in  $\text{Al}_2\text{O}_3$ , most likely part of the spinel phase which reduces the oxygen absorption/desorption values. As mentioned earlier, the spinel phase does not decompose in the redox reaction temperature. Also, X-ray map analysis shows that in addition to the concentration of aluminum in some places, this element has distributed in other parts of the sample and among cobalt oxide particles that can prevent the sintering of cobalt oxide particles during redox

process. Rod shape particles in Fig. 4, marked with C point, are free from Al and close to  $\text{Co}_3\text{O}_4$  composition. These rods probably grow during the re-oxidation step.

### 3.3. Effect of Mechanical Activation on $\text{Co}_3\text{O}_4$ -5wt. % $\text{Y}_2\text{O}_3$ Redox Behavior

Results of TG analysis of the yttria-containing samples are presented in Fig. 5. According to Fig. 5, the cycles are irregular and mechanical activation has significantly decreased the weight change value. As it is seen, the weight change of CY2, CY8, and CY16 is close to 2 wt. %, 1 Wt. %, and zero, respectively. It means that heat storage properties of CY samples are significantly less than as-received cobalt oxide. Information extracted from Fig. 6 are shown in Table 3. It is seen that with the increase in the activation time, the oxygen absorption/desorption values decrease, and finally the values reaches to zero in CY16 sample. Generally, according to Fig. 5 and Table 3, it is clear that increasing the activation time has led to



Fig.4. X-ray map and EDS analyses of CA8 sample after three redox cycles.



the loss of thermochemical heat storage properties of CY samples in comparison with as-received cobalt oxide. Most probably, the weak performance of yttria-containing samples is related to morphology and structure of particles.



Fig. 5. TG analysis of CY2, CY8 and CY16 samples.

Fig. 6 illustrates the SEM images and Table 4 shows the average particle size of CY2, CY8, and CY16 samples before and after three redox cycles. Average particle size of CY2, CY8, and CY16 before redox is 0.55, 0.98 and 0.63  $\mu\text{m}$ , respectively. Average particle size of mentioned samples after redox is 6.00, 7.40, and 5.25  $\mu\text{m}$ , respectively. Although, the average particle size has decreased by mechanical activation, but it intensively increases the sintering of the samples after redox (Fig.6). This increase in sintering reduces the absorption and desorption of oxygen as shown in Fig. 5. As a result, oxygen absorption and desorption in the CY16 sample was completely stopped.

Table 4. Average particle size of CY samples before and after redox

| Sample | Average particle size ( $\mu\text{m}$ ) |                      |
|--------|---|----------------------|
|        | before 3 redox cycles                   | after 3 redox cycles |
| CY2    | 0.55                                    | 6.00                 |
| CY8    | 0.98                                    | 7.40                 |
| CY16   | 0.63                                    | 5.25                 |

There are spherical particles (D points) in SEM images presented in Fig. 6. EDS and X-ray map analysis were used to investigate the particles composition and various element distributions. Results of the X-ray map and EDS analysis of CY8 sample after three redox cycle are shown in

Table 3. Weight change and it's rate during first to third cycles for yttria containing samples

| Sample code                         | Weight change wt. % |      |         |      |         |      | Weight change rate (wt. % / min) |      |         |      |         |      |
|-------------------------------------|---------------------|------|---------|------|---------|------|----------------------------------|------|---------|------|---------|------|
|                                     | Cycle 1             |      | Cycle 2 |      | Cycle 3 |      | Cycle 1                          |      | Cycle 2 |      | Cycle 3 |      |
|                                     | Red                 | Oxid | Red     | Oxid | Red     | Oxid | Red                              | Oxid | Red     | Oxid | Red     | Oxid |
| As-received $\text{Co}_3\text{O}_4$ | 4.20                | 4.20 | 3.40    | 2.20 | 1.80    | 0    | 0.37                             | 0.18 | 0.11    | 0.11 | 0.05    | 0    |
| CY2                                 | 1.84                | 1.84 | 2.09    | 2.09 | 1.58    | 1.58 | 0.35                             | 0.07 | 0.35    | 0.02 | 0.17    | 0.03 |
| CY8                                 | 1.15                | 1.15 | 1.32    | 1.32 | 1.05    | 1.05 | 0.04                             | 0.04 | 0.04    | 0.09 | 0.14    | 0.05 |
| CY16                                | 0                   | 0    | 0       | 0    | 0       | 0    | 0                                | 0    | 0       | 0    | 0       | 0    |



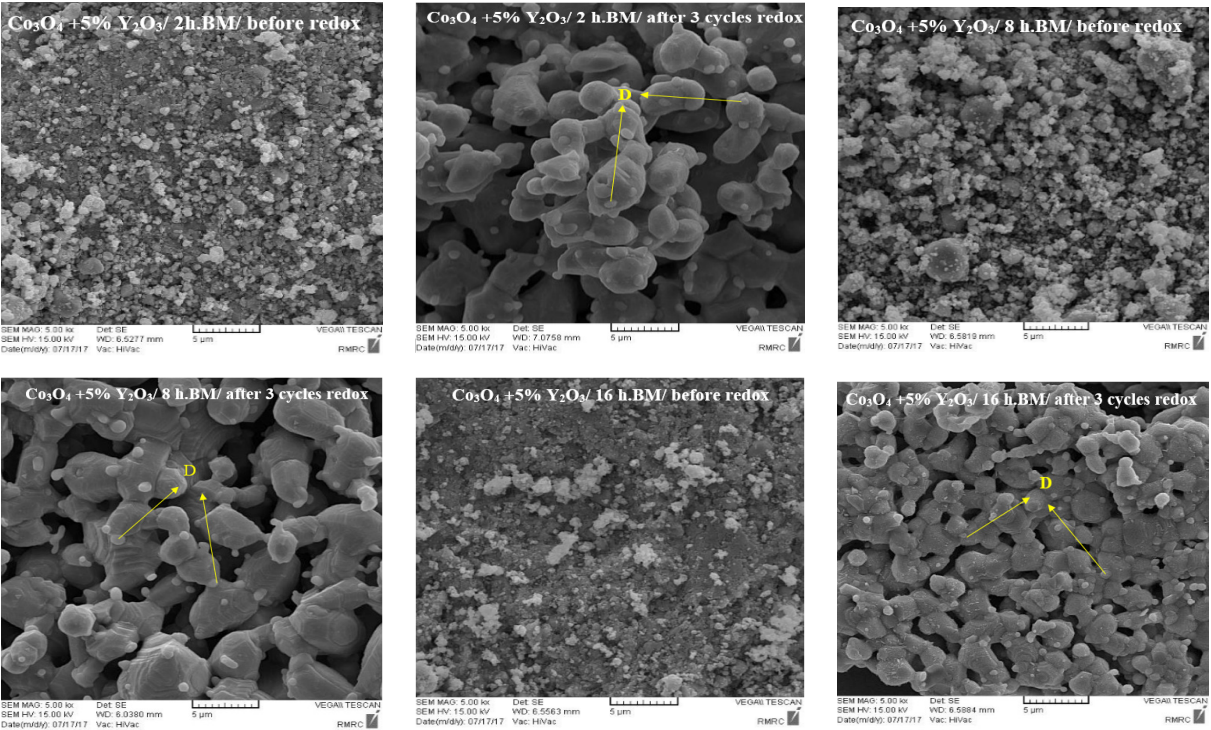


Fig. 6. SEM images of CY2, CY8 and CY16 samples before and after three redox cycles.



Fig. 7. X-ray map and EDS analyses of CY8 sample after three redox cycles.

Fig. 7. It is seen that yttrium oxide has distributed throughout the sample, but its concentration is higher at some points. These points are the same spherical particles shown with D points in Fig. 6 and they are a phase that is rich in yttrium oxide. It seems that yttrium oxide reacts with cobalt oxide and forms a new compound. Weak performance of  $\text{Co}_3\text{O}_4$ -5 wt. %  $\text{Y}_2\text{O}_3$  in view of thermochemical heat storage properties is related to intensive sintering, growth of cobalt oxide particles, and formation of new phases that do not decompose. In fact,  $\text{Y}_2\text{O}_3$  addition has intensively increased the sintering and growth of cobalt oxide particles. It seems that due to smaller ionic size of  $\text{Co}^{+3}$  and  $\text{Co}^{+2}$  relative to  $\text{Y}^{+3}$  ions, there is diffusion of cobalt ions into  $\text{Y}_2\text{O}_3$  surface and structure and  $\text{Y}_2\text{O}_3$  has not played any role in the prevention of cobalt oxide particles sintering.

### 3.4. Comparison of $\text{Y}_2\text{O}_3$ and $\text{Al}_2\text{O}_3$ Additives Performance

The addition of  $\text{Al}_2\text{O}_3$  improves the redox behavior of cobalt oxide, while the addition of  $\text{Y}_2\text{O}_3$  severely degrades the redox process. This difference in  $\text{Al}_2\text{O}_3$  and  $\text{Y}_2\text{O}_3$  performance is related to their effect on growth and sintering of cobalt oxide particles and also the formation of new phases. In fact,  $\text{Y}^{+3}$  cations due to higher atomic radius cannot diffuse to cobalt oxide structure, while  $\text{Co}^{+3}$  or  $\text{Co}^{+2}$  cations can diffuse into yttrium oxide structure.  $\text{Al}^{+3}$  cations due to smaller atomic radius can easily diffuse into the cobalt oxide structure. For this reason, as shown in SEM images (Fig. 3 and Fig. 6) the  $\text{Y}_2\text{O}_3$  particles unlike  $\text{Al}_2\text{O}_3$  particles not only do not disappear during redox process, but also their sizes have increased after redox reactions.

## 4. CONCLUSIONS

The following conclusions were obtained from this research work:

1. Alumina addition and mechanical activation have improved the reduction and re-oxidation kinetics of cobalt oxide in comparison with as-received cobalt oxide. Although, the samples activated for short time show better redox kinetics than samples activated for longer time.

2. Increasing the activation time to more than 8 h for alumina-containing samples reduces the thermochemical heat storage properties of  $\text{Co}_3\text{O}_4$  due to decrease in positive effect of additive in controlling the particle size growth and sintering.
3. X-ray map and EDS analysis showed that agglomerated particles in alumina-containing samples are rich in  $\text{Al}_2\text{O}_3$ , most likely part of the spinel phase which reduces the oxygen absorption/desorption values.
4. Oxygen absorption and desorption in yttria-containing sample activated for 16 h was completely stopped.
5. Weak performance of  $\text{Co}_3\text{O}_4$ -5 wt. %  $\text{Y}_2\text{O}_3$  in view of thermochemical heat storage properties is related to intensive sintering and growth of cobalt oxide particles.
6. The addition of  $\text{Al}_2\text{O}_3$  and mechanical activation up to 8 h improves the redox behavior of alumina-containing samples, while the addition of  $\text{Y}_2\text{O}_3$  and mechanical activation severely degrades the thermochemical heat storage properties of yttria-containing samples.

## ACKNOWLEDGMENTS

The authors are grateful to Mr. A. Nsari for his assistance in conducting the experiments. This work was supported by Hamedan University of Technology [Grant No. 18-94-1-361].

## REFERENCES

1. Shine, K. P., Fuglestedt, J. S., Hailemariam, K. and Stuber, N., "Alternatives to the Global Warming Potential for Comparing Climate Impacts of Emissions of Greenhouse Gases". *Clim. Change*, 2005, 68, 281–302.
2. Abedin, A. H. and Rosen, M. A., "A Critical Review of Thermochemical Energy Storage Systems". *Open Renew. Energy J.*, 2011, 4, 42–46.
3. Singh, A., Tescari, S., Lantin, G., Agrafiotis, C., Roeb, M. and Sattler, C., "Solar thermochemical heat storage via the  $\text{Co}_3\text{O}_4$  /CoO looping cycle: Storage reactor modelling and experimental validation". *Sol. Energy*, 2017, 144, 453–465.
4. Mehling, H. and Cabeza, L. F., "Heat and Cold Storage with PCM", 1<sup>st</sup> ed., Springer, Germany,

- 2008, 1-52.
5. Dincer, I., Rosen, M. A., "Thermal Energy Storage: Systems and Applications", 2<sup>nd</sup> ed., John Wiley & Sons, Canada, 2011, 83-187.
6. Sayigh, A., "Comprehensive Renewable Energy", 1<sup>st</sup> ed., Elsevier, UK, 2012, 1-25.
7. Tescari, S., Singh, A., Agrafiotis, C., Oliveira, L., Breuer, S., Schlögl-Knothe, B., Roeb, M. and Sattler, C., "Experimental evaluation of a pilot-scale thermochemical storage system for a concentrated solar power plant". Appl. Energy, 2017, 189, 66-75.
8. "Thermochemical Heat Storage for Concentrated Solar Power", Report of General Atomic Project No. 30314, U.S. Department of Energy, 2008.
9. Carrillo, A. J., Moya, J., Bayon, A., Jana, P., de la Pena Oshea, V. A., Romero, M., Gonzalez-Aguilar, J., Serrano, D. P., Pizarro, P. and Coronado, J. M., "Thermochemical energy storage at high temperature via redox cycles of Mn and Co oxides: Pure oxides versus mixed ones". Sol. Energy Mater. Sol. Cells, 2014, 123, 47-57.
10. Muroyama, A. P., Schrader, A. J. and Loutzenhiser, P. G., "Solar electricity via an air Brayton cycle with an integrated two-step thermochemical cycle for heat storage based on  $\text{Co}_3\text{O}_4/\text{CoO}$  redox reactions II: Kinetic analyses". Sol. Energy, 2015, 122, 409-418.
11. Block, T., Knoblauch, N. and Schmücker, M., "The cobalt-oxide/iron-oxide binary system for use as high temperature thermochemical energy storage material". Thermochim. Acta, 2014, 577, 25-32.
12. Hutchings, K. N., Wilson, M., Larsen, P. A. and Cutler, R. A., "Kinetic and thermodynamic considerations for oxygen absorption/desorption using cobalt oxide". Solid State Ionics, 2006, 177, 45-51.
13. Neises, M., Tescari, S., Oliveira, L. de, Roeb, M., Sattler, C. and Wong, B., "Solar-heated rotary kiln for thermochemical energy storage". Sol. Energy, 2012, 86, 3040-3048.
14. Pagkoura, C., Karagiannakis, G., Zygogianni, A., Lorentzou, S., Konstandopoulos, A. G., "Cobalt oxide based honeycombs as reactors/heat exchangers for redox thermochemical heat storage in future CSP plants". Energ Procedia, 2015, 69, 978-987.
15. Carrillo, A. J., Serrano, D. P., Pizarro, P. and Coronado, J. M., "Thermochemical Heat Storage at High Temperatures using  $\text{Mn}_2\text{O}_3/\text{Mn}_3\text{O}_4$  System: Narrowing the Redox Hysteresis by Metal Co-doping". Energy Procedia 2015, 73, 263-271.
16. Agrafiotis, C., Roeb, M., Schmücker, M. and Sattler, C., "Exploitation of thermochemical cycles based on solid oxide redox systems for thermochemical storage of solar heat". Part 1: Testing of cobalt oxide-based powders. Sol. Energy, 2014, 102, 189-211.
17. El-Eskandarany, M. S., "Mechanical alloying: Nanotechnology, Materials Science and Powder Metallurgy", 2<sup>nd</sup> ed., Elsevier, USA, 2015, 34-61.
18. Nekokar, N., Pourabdoli, M., Ghaderi Hamidi, A. and Uner, D., "Effect of mechanical activation on thermal energy storage properties of  $\text{Co}_3\text{O}_4/\text{CoO}$  system". Adv. Powder Technol., 2018, 29, 333-340.
19. Nekokar, N., Pourabdoli, M. and Ghaderi Hamidi, A., "Effect of  $\text{Fe}_2\text{O}_3$  Addition and Mechanical Activation on Thermochemical Heat Storage Properties of  $\text{Co}_3\text{O}_4/\text{CoO}$  System". J. Part. Sci. & Technol., 2018, 4, 13-22.
20. Block, T. and Schmücker, M., "Metal oxides for thermochemical energy storage: A comparison of several metal oxide systems". Sol. Energy, 2016, 126, 195-207.
21. Patnaik, P., Handbook of Inorganic Chemicals, 1<sup>st</sup> ed., McGraw-Hill, USA, 2003, 231-252.